

Concept of Community Fragilities for Tsunami Coastal Inundation Studies

Sangki Park¹; John W. van de Lindt, M.ASCE²; Daniel Cox, M.ASCE³; and Rakesh Gupta, M.ASCE⁴

Abstract: Tsunamis have devastated coastal regions worldwide, with the most recent being the result of the Great Tohoku Japan earthquake and tsunami, which was a M9.0 undersea megathrust earthquake that occurred off the east coast of Japan on March 11, 2011. In this study, a fragility formulation is utilized to develop and illustrate the concept of community fragilities for a community subjected to a wave of a particular height because fragilities are independent of occurrence rate. The fragility formulation for single structures is explained and then extended to the community scale by assigning one of eight archetype structural models and corresponding fragility to each of the buildings in a community. One key feature of the approach is that both the earthquake and tsunami are considered in succession. Three wave forces, i.e., hydrostatic, hydrodynamic, and impulsive wave forces, and the successive hazard loadings, i.e., earthquakes and tsunamis, were considered during the analysis. While debris loading is often critical during inundation, it is not assessed here but should be eventually considered. The tsunami fragility methodology is briefly demonstrated on a single building and then extended to Cannon Beach, Oregon, as an illustrative example. The fragility approach shows that community fragilities follow a similar trend with single structure fragilities and can help with decision making for retrofit and land-use planning. The concept proposed herein can provide a framework regardless of the structural or hydrodynamic model used, provided information on the community is available and a basic understanding of the structure types can be developed. DOI: [10.1061/\(ASCE\)NH.1527-6996.0000092](https://doi.org/10.1061/(ASCE)NH.1527-6996.0000092). © 2013 American Society of Civil Engineers.

CE Database subject headings: Tsunamis; Coastal environment; Earthquakes; Decision making; Floods; Community development.

Author keywords: Tsunami; Fragility; Coastal inundation; Earthquake; Combined hazard; Community risk; Decision making.

Introduction

The understanding of tsunami generation, propagation, and inundation has improved significantly over the last 10–20 years, but there has been less progress on understanding the interaction between tsunamis and structures during overland flow and return. A method to estimate the fragility of a community located in a potential tsunami inundation zone can provide emergency planners information on the likely number of structural failures as a function of tsunami height as well as provide engineers a method for calibrating design codes based on community needs rather than just an individual building failure probability. Thus, this paper should be of interest to engineers and emergency planners with an emphasis on natural hazards. The FEMA P646 guidelines (FEMA 2008) recommend considering both the earthquake demand from shaking and the tsunami demand for the design of vertical evacuation structures in certain coastal regions such as the U.S. Pacific Northwest. While this

may not be current practice in most areas, it is important to develop a better understanding of how one hazard affects the other because the hazards would typically occur rapidly in succession, i.e., without the ability to repair between loadings. Building design codes are based on load occurrence probability and resistance statistics of the components making up a building system, but tsunamis are typically not considered in design except in very rare circumstances and are not considered in woodframe design.

Clearly, the design of coastal structures in a tsunami-hazard zone should take into account loading from tsunamis if the structure is to be considered safe for use as a vertical evacuation facility. Structural damage from tsunamis is caused by water-borne debris and direct hydrostatic, and in particular hydrodynamic, forces. In this paper, only hydrostatic and hydrodynamic loads are examined, but it is noted that loads caused by water-borne debris are often critical and must eventually be taken into account as more research is performed related to their occurrence rates and mechanisms of loading on structures. Experimental and numerical studies (e.g., Neelamani et al. 1999; FEMA 2008; Wilson et al. 2009) or incident wave conditions (Ramsden 1996; Linton et al. 2011) demonstrate that the wave forces exerted on a structure are directly related to wave height and speed.

The ASCE Standard 7 (ASCE 2010) has proposed equations based on fluid mechanics and experimental test data. The FEMA P646 guidelines (FEMA 2008) state that tsunami wave forces should be considered for the design of coastal structures, especially vertical evacuation structures. This approach provides an equivalent force expressed as a function of tsunami inundation height. There have been many recent advances in tsunami-structure interaction models but this area of research still lags behind more established research related to wave impact on maritime offshore structures or coastal structures (e.g., Goda 2010). Thus, this study

¹Postdoctoral Scholar, Dept. of Civil, Construction, and Environmental Engineering, Univ. of Alabama, Tuscaloosa, AL 35487-0205. E-mail: skpark@eng.ua.edu

²George T. Abell Professor of Infrastructure, Dept. of Civil and Environmental Engineering, Colorado State Univ., Fort Collins, CO 80523-1372 (corresponding author). E-mail: jwv@engr.colostate.edu

³Professor, School of Civil and Construction Engineering, Oregon State Univ., Corvallis, OR 97331.

⁴Professor, Dept. of Wood Science and Engineering, Oregon State Univ., Corvallis, OR 97331.

Note. This manuscript was submitted on January 6, 2012; approved on August 28, 2012; published online on September 1, 2012. Discussion period open until April 1, 2014; separate discussions must be submitted for individual papers. This paper is part of the *Natural Hazards Review*, Vol. 14, No. 4, November 1, 2013. ©ASCE, ISSN 1527-6988/2013/4-220–228/\$25.00.

uses the formulas proposed in FEMA P646 (FEMA 2008) to compute tsunami wave forces for illustrative purposes with the caveat that they are approximations.

In earthquake engineering, probabilistic relationships between structural damage and earthquake ground motion intensity are known as fragility curves. Fragility curves describe the conditional probabilities of sustaining different degrees of damage at given levels of ground motion intensity. Thus, the development of fragility curves and damage probability matrices requires the characterization of ground motion and the identification of different degrees of structural damage. Shinozuka et al. (2000) presented a statistical analysis of structural fragility curves for both empirical and analytical approaches. They utilized bridge damage data obtained from the 1995 Kobe earthquake for constructing fragility curves. Rosowsky and Ellingwood (2002) and Ellingwood et al. (2004) developed a fragility analysis methodology for assessing the response of light-frame wood construction exposed to extreme windstorms and earthquakes. Park and van de Lindt (2009) developed a fragility formulation that provided a method to assess the seismic vulnerability of a structure using existing shake table test data. A performance-based wind engineering approach was built on the logic of the Ellingwood et al. (2004) study and was based on the fragility curves proposed by van de Lindt and Dao (2009). Koshimura et al. (2009b) applied a fragility analysis for a tsunami hazard based on numerical simulations, observations, and data from the 2004 Indian Ocean tsunami disaster. Although the previously cited studies are just a handful of recent fragility studies, they highlight the diversity of fragility development and application.

Loading and Structural Response Modeling

Tsunami Loading

The FEMA P646 guidelines (FEMA 2008) and USGS (2011) define their own tsunami terminology qualitatively and quantitatively. Clear terminology related to tsunamis is imperative to form a clear understanding of the problem at hand. Tsunami inundation height or depth is the vertical distance between the elevation of the highest local water mark at the structure and the elevation of the ground level at the time of the tsunami. The run-up height is taken to be the vertical distance from a datum, e.g., mean sea level (MSL), to the maximum point of run-up. By definition, the inundation height is 0 at the point of maximum run-up. Also, local run-up height is introduced and defined as the run-up height at the location of the structure. Fig. 1

depicts the physical meanings of the terms used throughout this study.

The FEMA P646 guidelines (FEMA 2008) define eight different types of forces that can potentially act on a structure during a tsunami, three of which are considered for illustration herein: (1) hydrostatic forces, (2) hydrodynamic forces, and (3) impulsive forces. It should be noted that buoyancy can contribute to the uplift failure of a structure, but this study focuses on shear failure of the structure and thus neglects buoyancy. The other forces, such as debris forces, were felt to be beyond the scope of this work but the authors are aware of at least one project that is underway by other researchers to experimentally evaluate debris impact forces on columns. A hydrostatic force acts when standing or slowly moving water is against a structure and can be computed as

$$F_h = \frac{1}{2} \rho_s g B h^2 \quad (1)$$

where ρ_s = fluid density including sediment $1,200 \text{ kg/m}^3 = 2.33 \text{ slugs/ft}^3$; g = gravitational acceleration; B = width of the structure or structural component; and h = maximum water height, i.e., inundation height, above the base of the wall at the structure location and less than the height of the structure for this study.

It should be noted that local run-up height on a structure is not used in this study. Rather, it is assumed that the inundation on a structure is based on the maximum run-up height at the furthest point inland. Of course, it is possible to compute it accurately through detailed numerical simulation, e.g., COBRAS (Liu 2009) and FUNWAVE (Kirby 2009), but requires computational effort beyond the objectives of this study. Fig. 2 shows the assumed run-up height and effect on the community.

In the analysis, the tsunami is assumed to occur, although the occurrence probability is not considered, and then the tsunami run-up height is investigated for heights ranging from 0 to a specified height, i.e., 50 m for the community example herein. A coefficient of variation (COV), i.e., the ratio of standard deviation to the mean, is included in the analysis which provides the height variation to be included in the analysis. Then, the inundation height for a structure is computed from the tsunami run-up height. Fragilities are conditional on occurrence of the hazard and thus a range of tsunami run-up heights can be investigated and later coupled with the occurrence probability of a tsunami as a function of the specific location.

When water flows around a structure, the hydrodynamic force can be computed using Eq. (2)

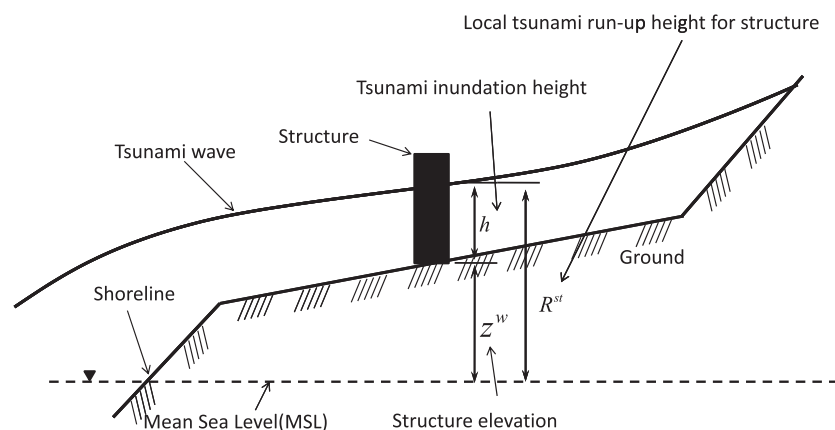


Fig. 1. Schematic explanation of tsunami terminology

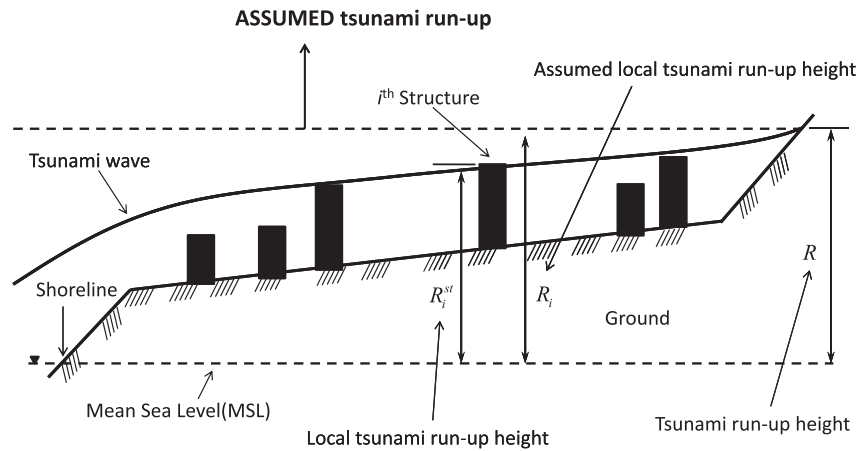


Fig. 2. Assumed tsunami run-up height for community

$$F_d = \frac{1}{2} \rho_s C_d B (hu^2)_{\max} \quad (2)$$

where ρ_s = fluid density including sediment $1,200 \text{ kg/m}^3 = 2.33 \text{ slugs/ft}^3$; C_d = drag coefficient; B = width of the structure in the plane normal to the direction of flow; h = flow depth termed tsunami inundation height for clarity this study; and u = flow velocity at the location of the structure.

Impulsive forces are caused by the leading edge of a surge of water impacting a structure. It is conservatively recommended that the impulsive force be taken as 1.5 times the hydrodynamic force as $F_s = 1.5F_d$.

Detailed explanations of these three forces can be found in FEMA P646 (FEMA 2008). Thus, the tsunami wave force can be computed as the summation of these three forces and expressed as

$$T_{tot} = F_h + F_d + F_s \quad (3)$$

where T_{tot} = total tsunami wave force; F_h = hydrostatic force; F_d = hydrodynamic force; and F_s = impulsive force.

Structural Modeling

To determine the effect of the earthquake and tsunami, a numerical model of a building that has the capability to degrade in both

stiffness and strength is needed. The Consortium of Universities for Research in Earthquake Engineering (CUREE) model, also known as the modified Stewart model, was refined as part of the CUREE Caltech Woodframe research project and is selected for use in the current study. Initially, Folz and Filiatrault (2001) modified the exponential envelop curve used by Dolan (1989) to include hysteretic characteristics of a Stewart model (1987). Hysteretic characteristics define a hysteresis that is used to model all or part of a building or other structure in earthquake engineering and, specifically, often allow the model to better represent damage during an earthquake. The CUREE model has been employed to simulate the shear behavior of single sheathing-to-framing fasteners in wood shear walls and an equivalent single-degree-of-freedom (SDOF) model for entire wood shear walls.

A force-deformation response of a sheathing-to-framing connector has highly nonlinear behavior under monotonic and cyclic loading. Initially, as loading is increased, the connector deforms and its connection starts losing capacity because the connector gradually crushes the wood fibers. Fig. 3(a) shows the force-deformation curve under monotonic loading. Eq. (4) presents the mathematical expression for a sheathing-to-framing connector deforming in shear, which captures the crushing between the wood framing and sheathing as well as yielding of the connector

$$P = \begin{cases} \text{sign}(\delta)(P_0 + r_1 K_0 |\delta|) [1 - \exp(-K_0 |\delta| / P_0)] & : |\delta| \leq |\delta_u| \\ \text{sign}(\delta) P_u + r_2 K_0 [\delta - \text{sign}(\delta) \delta_u] & : |\delta_u| < |\delta| \leq |\delta_F| \\ 0 & : |\delta| > |\delta_F| \end{cases} \quad (4)$$

where K_0 = initial stiffness; P_0 = initial force; r_1 = secondary stiffness factor; r_2 = tertiary stiffness factor; δ_u = ultimate displacement; and δ_F = failure displacement defined as the displacement that occurs when the connector fails.

Earthquake Loading

In an earthquake, the loading goes through full reversals, i.e., cyclic loading, and thus the connector behaves as a pinched hysteresis loop. During reversed-cyclic loading, hysteretic behavior is idealized by

using a predefined set of load paths to describe loading, unloading, and reloading. Initially, the loading rules follow the monotonic backbone curve described previously. Unloading rules can be defined as piecewise linear segments using two degrading stiffnesses, $r_3 K_0$ and $r_4 K_0$. During unloading, the connector loses partial contact with the surrounding wood due to permanent deformation caused by previous loading. Reloading after unloading exhibits a pinching stiffness K_p , where the pinching force P_l corresponds to 0 displacement and the reversal load path follows the unloading stiffness. The stiffness and strength degradation are defined using Eq. (5)

$$K_P = K_0 \left(\frac{P_0}{\beta K_0 \delta_{UN}} \right)^\alpha \quad (5)$$

$$F = P[D \geq C|I] \quad (6)$$

where K_0 = initial stiffness; F_0 = initial force; α and β = stiffness degradation parameters; and δ_{UN} = last unloading displacement. The CUREE model, depicted in Fig. 3(b), can be defined as a function of the 10-parameter hysteretic model with loading and unloading rules.

Fragility Formulation and Application

Fragility Formulation

A fragility curve is a conditional statistical distribution that gives the probability of exceeding a specified threshold or achieving a specific condition, e.g., drift, damage, or collapse, as a function of hazard intensity. For earthquake hazard, intensity can be expressed in terms of spectral acceleration. For structures in the inundation zone, the tsunami hazard intensity can be selected based on factors such as inundation height, velocity, or a combination of parameters describing the resulting wave force (Koshimura et al. 2009a). Moreover, the wave forces and height are clearly linked with each other. The wave height was selected as the measure of hazard intensity for the tsunami. Thus, it is proposed herein that tsunami fragility will define the conditional probability of the demand (D) of the wave forces placed upon the structure exceeding the structural capacity (C) for a given level of tsunami intensity (I) and can be expressed as

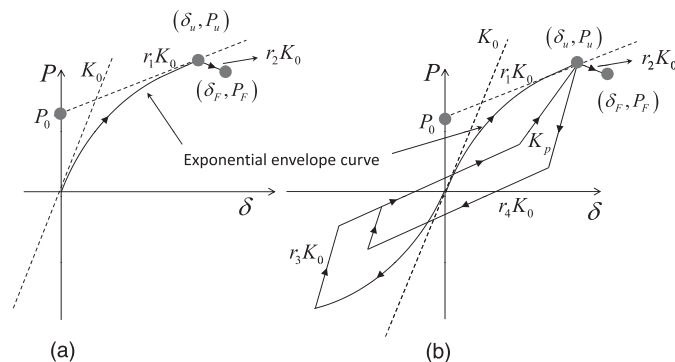


Fig. 3. Force-deformation curve of CUREE model: (a) monotonic loading case; (b) cyclic loading case

where F represents the fragility.

Generally, the lognormal distribution (Shinozuka et al. 2000; Ellingwood 2001; Rosowsky and Ellingwood 2002; Koshimura et al. 2009a, b; Park and van de Lindt 2009) is a convenient way to express a fragility and can be expressed as

$$F_R(x) = \Phi \left(\frac{\ln(x) - m_R}{\xi_R} \right) \quad (7)$$

where $\Phi(\cdot)$ is a standard normal distribution function; x = spectral acceleration or tsunami wave height; m_R = logarithmic mean; and ξ_R = logarithmic standard deviation.

This study focuses on the successive hazard of earthquakes and tsunamis; thus, the spectral acceleration (S_a) and tsunami inundation height (h) are selected as the x variable in Eqs. (6) or (7) for seismic and tsunami hazard, respectively.

Single Structure Fragilities

Prior to computing the collapse fragility from tsunami loading, a nonlinear time history analysis for the earthquake that may have produced the tsunami is performed. Fig. 4 provides a schematic overview of the two-stage analysis procedure used in this study, and Park et al. (2012) developed the general shape of a fragility from this two-stage analysis. The tsunami loading characterized by FEMA P646 (FEMA 2008) is used in the second stage of the analysis.

In this study, the issues of occurrence rate, i.e., tsunami hazard level, are not addressed. Rather, it is assumed that the tsunami occurs and the collapse probabilities are computed. Recall that this is one advantage of fragilities; namely, they are developed independently from the hazard or occurrence rate, essentially making them general and applicable to different sites provided they are eventually recoupled with the occurrence probability at a given site through convolution. Approximate tsunami wave loading can be computed using the set of force equations proposed in FEMA P646 (FEMA 2008), as discussed earlier.

In Stage 2 of the analysis procedure, a nonlinear static pushover analysis is performed using these computed tsunami loads based on the tsunami inundation height under investigation. A nonlinear static pushover analysis is a procedure in which a horizontal load is numerically applied at the top of a building model. It is incrementally increased, and at each increment, the stiffness matrix is recomputed to account for the building damage as modeled by the hysteresis. The result is as if one is actually pushing over a building, hence the name.

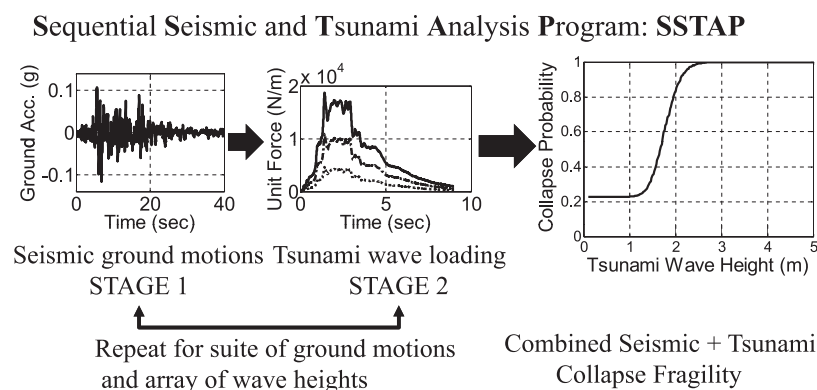


Fig. 4. Schematic overview of 2-stage analysis procedure used in this study

The computed tsunami forces are converted into an equivalent force and then applied to the SDOF system at the top of the wall. If the computed tsunami loading exceeds the structural capacity, the structure is assumed to have collapsed. The equivalent force at the top of the wall is computed using basic force equilibrium to ensure it has the same effect that the FEMA P646 (FEMA 2008) forces would impose. Park et al. (2012) provides further details.

For the seismic analysis, two seismic intensity levels described in terms of spectral acceleration, which are commonly used in design and analysis, are design basis earthquake (DBE) and maximum credible earthquake (MCE), representing 10 and 2% exceedance probabilities in 50 years, respectively (ASCE 2010). All 44 ground motions (the 22 pairs summarized in Table 1) were used in Stage 1 of the analysis for 44 earthquake analyses at each intensity level to represent the uncertainty in earthquake intensity. Then, using the damaged numerical model, which was numerically represented by maintaining the stiffness and strength degradation and future reloading path in the hysteretic springs, the tsunami analysis was performed to check the collapse of the structure under given inundation heights. Variation in the inundation heights was introduced by applying a range of COVs.

The tsunami inundation heights were generated in 0.1-m increments from 0.0 to 5.0 m. Each of these was treated as the mean tsunami inundation height for that analysis and the COV used to introduce dispersion about the mean. A lognormal distribution was assumed for the tsunami inundation height because lognormal distributions have been used extensively to introduce dispersion for other natural hazards and are used in fragility analysis. The COV for tsunami inundation heights was computed from the publicly accessible data described by Baldock et al. (2009) as 0.136 and is included as one of the COV values in the current study. That 13.6% variation was observed in a laboratory environment at Oregon State University where the tsunami was generated with the same input conditions to the wavemaker and the wave basin topography was

Table 1. Summary of TC-63's 22 Ground Motions (Excerpted from FEMA 2009)

Identity number	Earthquake			Peak ground acceleration (g)	
	M	Year	Name	Component1	Component2
1	6.7	1994	Northridge	0.42	0.52
2	6.7	1994	Northridge	0.41	0.48
3	7.1	1999	Duzce, Turkey	0.73	0.82
4	7.1	1999	Hector Mine	0.27	0.34
5	6.5	1979	Imperial Valley	0.24	0.35
6	6.5	1979	Imperial Valley	0.36	0.38
7	6.9	1995	Kobe, Japan	0.51	0.50
8	6.9	1995	Kobe, Japan	0.24	0.21
9	7.5	1999	Kocaeli, Turkey	0.31	0.36
10	7.5	1999	Kocaeli, Turkey	0.22	0.15
11	7.3	1992	Landers	0.24	0.15
12	7.3	1992	Landers	0.28	0.42
13	6.9	1989	Loma Prieta	0.53	0.44
14	6.9	1989	Loma Prieta	0.56	0.37
15	7.4	1990	Manjil, Iran	0.51	0.50
16	6.5	1987	Superstition Hills	0.36	0.26
17	6.5	1987	Superstition Hills	0.45	0.30
18	7.0	1992	Cape Mendocino	0.39	0.55
19	7.6	1999	Chi-Chi, Taiwan	0.35	0.44
20	7.6	1999	Chi-Chi, Taiwan	0.47	0.51
21	6.6	1971	San Fernando	0.21	0.17
22	6.5	1976	Friuli, Italy	0.35	0.31

nominally identical. Thus, neglecting variation in the wavemaker itself, it was assumed that when randomness in nature is introduced, the COV is larger, i.e., 13.6% is a lower bound.

The community-level example focuses on Cannon Beach, Oregon, a city in the Pacific Northwest of the United States. According to the USGS (2011), the DBE and MCE for Cannon Beach have spectral accelerations of 0.89 and 1.34g ($T_n = 0.2$ s; $\xi = 5\%$), respectively. These spectral acceleration levels are specific to this latitude and longitude and would change depending on the site being investigated. In the case of Cannon Beach, the primary hazard is from the Cascadia subduction fault, which is not considered a near fault and is located off the coast in the Pacific Ocean.

A 2-story light-frame wood structure was selected as an illustrative example. Each component of the building was modeled using the 10-parameter CUREE hysteresis model described earlier. The building was one unit of a 2-story townhouse, and its total living area was approximately 167 m² (1,800 ft²), with an attached two-car garage. The exterior walls of the 2-story example structure were covered on the outside with 22.23-cm (7/8-in.)-thick stucco over 11.12-cm (7/16-in.)-thick oriented strand board (OSB) sheathed shear walls, and 12.7-cm (1/2-in.)-thick gypsum wall-board (drywall) was on the inside. The capacity was based on that of a typical Pacific Northwest design. There are 24 wood shear walls, with 13 shear walls assigned for the first story and 11 shear walls for the second story. Each shear wall is represented by a single hysteretic spring element and provides resistance only in the shear direction, i.e., the transverse strength of the shear walls is neglected but is assumed to transfer tsunami loads to the shear walls oriented parallel to the direction of wave propagation.

Fig. 5 shows the results of three analyses. Specifically, the solid line represents the resulting collapse fragility when only the tsunami (no earthquake) is considered, the dash line represents the resulting collapse fragility when the DBE level earthquake and tsunami are both considered, and the dashed-dotted line represents the resulting collapse fragility when the MCE level earthquake and tsunami are considered. From the fragility, one can read that a 1.97-m inundation height will collapse the building 50% of the time, whereas a 1.67-m inundation height will collapse the building 50% of the time if subjected to the MCE level earthquake first. While this may seem a minimal difference at first inspection, it considers the lower bound

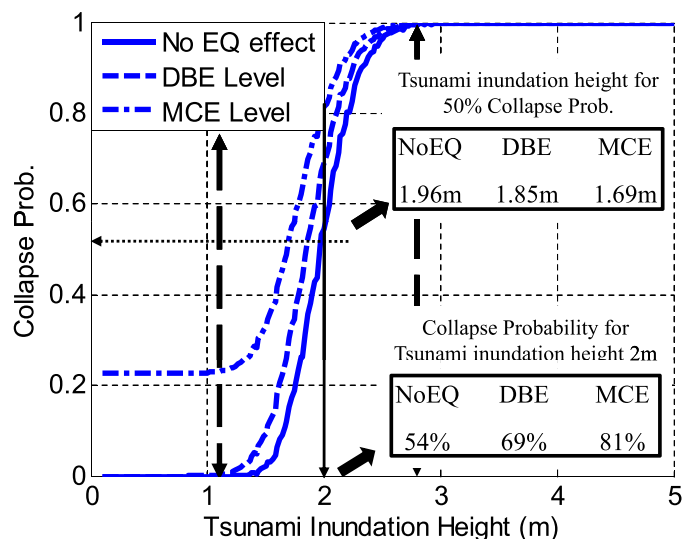


Fig. 5. Collapse probability of 13.6% COV for x -direction impact with 2-story building

coefficient of variation (COV) wave height. It should be noted that Eq. (6) was used to do a fragility analysis rather than Eq. (7). Generally, Eq. (7) is a more convenient expression than Eq. (6). However, Eq. (7) cannot express the fragility trend well when the fragility does not start at 0, e.g., the MCE level earthquake intensity is assumed to have occurred, which produces a horizontal lower tail.

In Fig. 5, the lower portion of the fragility is the earthquake sensitive section, i.e., at the MCE level, there is a 22% chance of the earthquake collapsing the building prior to the tsunami reaching the shore according to the model. Although these inundation heights are not large, the run-up height of the tsunami itself can be quite high. Regardless, the methodology for successive earthquake-tsunami analysis is one of the main focuses of this study and has applicability across a range of building materials and inundation heights.

From these basic results, one can observe that the tsunami inundation heights required to collapse a light-frame wood building decreased when the seismic intensity of the preceding earthquake increased. The difference is not as notable as one might anticipate, but the trend is evident. The methodology presented herein could be used to statistically determine requirements for vertical evacuation structures located in regions where near-field tsunamis are a risk, such as the U.S. Pacific Northwest. At this point, the methodology presented makes it possible to extend the fragility formulation to whole communities, provided the building elevations and types are known throughout the area of interest.

Community Fragilities

In previous sections, the tsunami framework for a single structure was developed and explained in detail. The objective of this study is to present a methodology and procedure for the development of a tsunami fragility framework and its extension to a coastal community. To do this, the community can be expressed as a combination of each building; thus, community fragility can also be

constructed as a weighted summation of single structure fragilities. The relationships can be expressed by introducing a summation

$$F_c = \sum_{i=1}^n \lambda_i^b F_i^b \quad (8)$$

where F_c = fragility for the community; F_i^b = fragility for the i th building; n = number of total buildings in the community; and λ_i^b is a weighting factor defined as

$$\lambda_i^b = \frac{I_i^b}{\sum_{i=1}^n I_i^b} \quad (9)$$

where λ_i^b = weighting factor for the j th building; and I_i^b is an importance parameter for the i th building and can be used to account for the number of people living in the buildings, the overall area of the buildings, and the importance of the building in the community, which could be used for hospitals, schools, fire stations, and police stations. Fig. 6 shows a schematic overview of the construction of the community fragilities from the combination of each single assembly.

The location of each single assembly in the community is an important factor because of the link among the tsunami wave forces, i.e., a house can have no damage from the tsunami if its location is far from the shoreline or at a high elevation. Thus, the proposed approach explained in the previous section can be applied directly to each single assembly and then individual fragilities can be obtained. Then, Eq. (8) calculates the community fragilities.

Illustrative Examples

The city of Cannon Beach along the northern Oregon coast was selected as an illustrative example and shown in Fig. 7 (City of

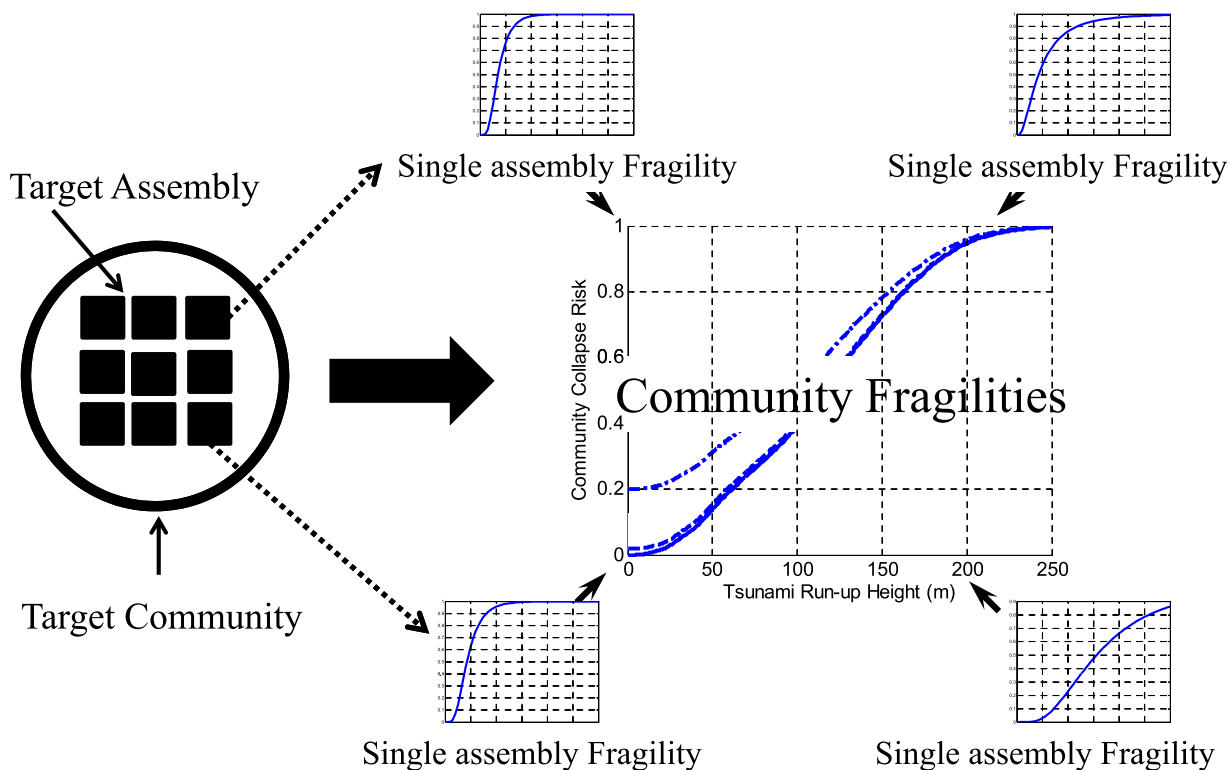


Fig. 6. Schematic overview of constructing community collapse risk fragilities

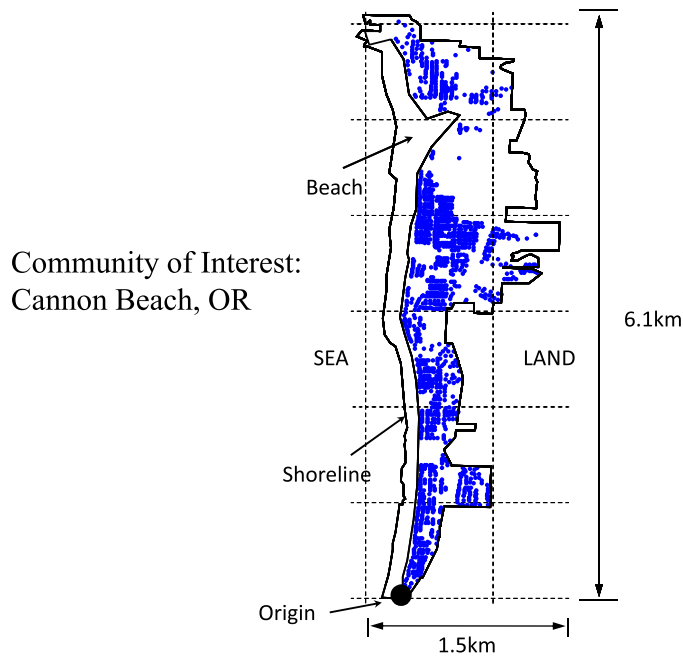


Fig. 7. City of Cannon Beach, Oregon

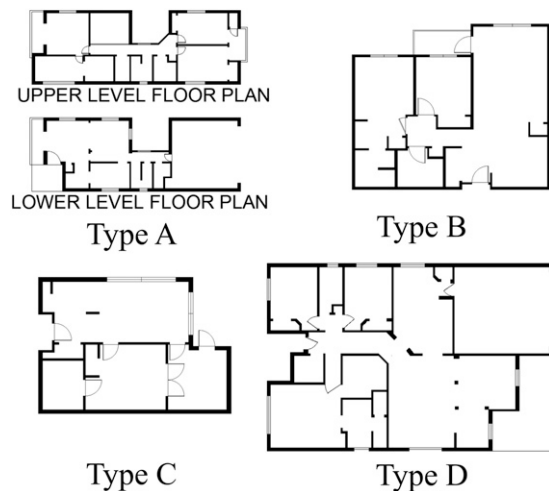


Fig. 8. Floor plan of four archetypes

Cannon Beach 2012). Residential structures are only considered in constructing the community fragilities for simplicity. Initially, the location of each house in Cannon Beach was computed based on a map image using the southwest corner of the boundary of the city limitation, i.e., the origin. The elevations were determined based on slope and distance from the shoreline.

In Fig. 7, the black solid line shows the boundary of the city, and dots represent approximately 1,400 individual houses for which detailed information is provided by Park (2011). To model the variety of house configurations in the community, three more residential houses having different floor plans are considered and analyzed using the proposed approach under the same conditions of successive earthquake and tsunami analysis. The number of shear walls in the house is based on the floor plan, and the capacities are based on typical Pacific Northwest construction. Together, this suite of archetypes was felt to provide a reasonable representation of the residential community.

Table 2. Structural Properties of Four Archetypes

Identity	Area (m ² /ft ²)	Weight (metric tons/kips)	Narrow width (m/ft)	Wide width (m/ft)
A	167.2/1,800.0	36.3/80	6.7/22.0	18.6/61.0
B	113.5/1,222.0	20.0/44.1	10.4/34.0	12.3/40.5
C	57.2/616.0	10.0/22.0	6.7/22.1	9.4/31.0
D	275.5/2,965.3	48.6/107.0	14.1/46.1	21.3/70.0

Table 3. Possible Eight Styles of Residential Building Type for Community

Style identity number	Residential building		Allocated number of style
	Structure type	Direction of wave	
1	A	x	101
2		y	190
3	B	x	187
4		y	207
5	C	x	216
6		y	220
7	D	x	212
8		y	89

Table 4. Collapse Probability from Only Earthquake Hazards

Style identity number	Collapse probability (%)	
	DBE level	MCE level
1	~0	22.73
2	~0	9.10
3	~0	22.73
4	~0	15.91
5	~0	15.91
6	9.10	34.10
7	~0	13.64
8	6.82	34.10

House Type A is the same house that was used in the previous single structure example and is shown in Fig. 8. Fig. 8 shows the floor plans for each of the archetypes, and Table 2 provides a summary of the details for each of these houses. Each building, i.e., the four archetype structures such as Types A, B, C, and D, could be loaded in either the narrow or broader building direction, i.e., the x- and y-directions of the house depending on the orientation of the building to the shoreline. Thus, eight different types of residential buildings were best matched to each building in the satellite images for use in the community-level fragility analysis and are shown in Table 3.

Fragility analysis was conducted for each of these structures similar to what was presented for the 2-story house earlier. Community fragilities were then constructed for each of these structures for the two COV values for wave height, i.e., 13.6 and 50.0%. Forces are computed from the tsunami inundation heights for each structure depending on its location and elevation. Each residential building has a collapse probability that was computed from the earthquake hazard similar to an initial condition, i.e., DBE or MCE level earthquake intensity is considered. This means that the community also has a seismic collapse vulnerability, i.e., at a certain level, DBE or MCE level, earthquake occurs. Thus, the collapse probability from the earthquakes is tabulated in Table 4 for clarity.

Fig. 9(a) presents community fragilities from the combination of the single structure fragilities when a 13.6% COV is applied to

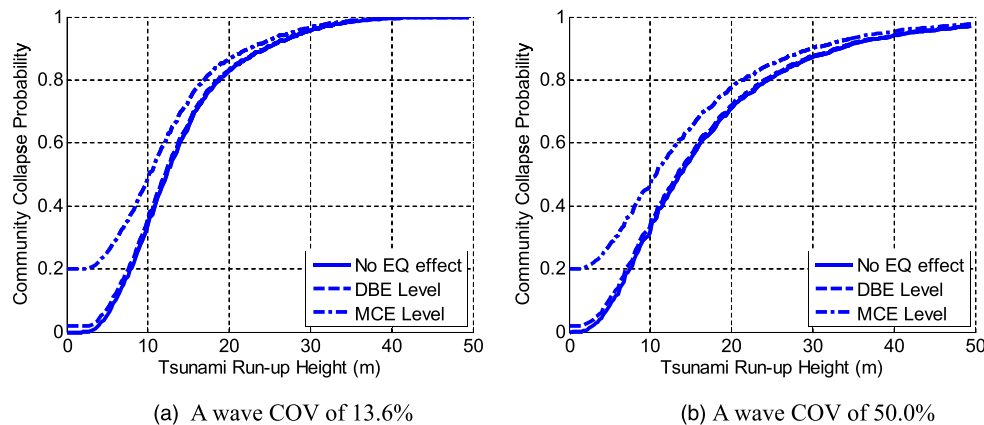


Fig. 9. Fragilities for community: (a) wave COV of 13.6%; (b) wave COV of 50.0%

generate the tsunami inundation data. The solid line represents the resulting collapse fragility when only the tsunami (no earthquake) is considered; the dashed line represents the resulting collapse fragility when the DBE level earthquake intensity and tsunami are considered; and the dashed-dotted line represents the resulting collapse fragility when the MCE level earthquake intensity and tsunami are considered in succession.

From the figures, the collapse probability from the earthquake hazard can be seen at the DBE and MCE level as 2 and 20%, respectively. The interpretation of this plot is as follows: a tsunami run-up height of 10 m would result in a 34, 36, and 49% collapse probability for a situation in which there was no earthquake shaking (only a tsunami), a DBE level earthquake produced the tsunami, or a MCE level earthquake produced the tsunami, respectively.

Recall that the x -axis in the figures is the tsunami run-up and not the tsunami inundation height, and is therefore a function of the elevation of the building, not just the structural properties. The reason is that each house is subjected to a different tsunami inundation height, typically defined as the vertical distance from the mean water elevation to the bottom of the structure, which is a function of their location in the community and topography. Thus, the tsunami run-up was felt to be a more reasonable variable to express the community fragilities.

Now, consider the fragilities for the same community but for a wave having a 50.0% COV, which may be more realistic based on the dearth of research on the relationship between earthquakes and the tsunamis they generate. Fig. 9(b) presents the collapse probabilities. One can see that if a tsunami is expected to be only 10 m, then the collapse probability is 32, 33, and 46% for the earthquake only, DBE level earthquake and tsunami, and MCE level earthquake and tsunami, respectively. In general, the overall collapse probability is not sensitive to the run-up COV except as the run-up becomes large.

Summary and Conclusion

Single structure fragilities were obtained by subjecting a structure to a suite of earthquake ground motions. After each motion, the numerically damaged structural model was subjected to nonlinear pushover analysis with equivalent tsunami wave loading. The approach was then extended to the community level, i.e., the community fragility was constructed as a weighted summation of the single structure fragilities. Both the single structure cases and the community analyses were presented in terms of fragilities as a function of the parent earthquake intensity level and tsunami run-up height. The development of collapse fragility curves for subsequent

earthquake and tsunami load can provide information needed to assess the vulnerability of the structures and community in near-field regions. It is these near-field regions that are (1) prone to ground shaking and (2) have insufficient tsunami warning time for evacuation because of the proximity of the offshore fault. The intent was that the concept proposed herein can provide a framework regardless of the structural or hydrodynamic model used, provided information on the community is available and a basic understanding of the structure types can be developed. The community fragility methodology can be applied by city and regional planners to determine where to focus limited financial resources for hazard mitigation.

Acknowledgments

The material presented in this paper is based upon work supported by the National Science Foundation under Grant No. CMMI-0830378 [George E. Brown, Jr. Network for Earthquake Engineering Simulation (NEES) Research] and CMMI-0402490 (NEES Operations). Any opinions, findings, and conclusions or recommendations expressed in this material are those of the author(s) and do not necessarily reflect the views of the National Science Foundation. The first and second authors also acknowledge partial contribution from Drummond Chair funds at the University of Alabama.

References

- ASCE. (2010). "Minimum design loads for buildings and other structures." *ASCE/SEI 7-10*, Reston, VA.
- Baldock, T. E., Cox, D., Maddux, T., Killian, J., and Fayler, L. (2009). "Kinematics of breaking tsunami wavefronts: A data set from large scale laboratory experiments." *Coastal Eng.*, 56(5–6), 506–516.
- City of Cannon Beach Oregon. (2012). "A map of the City of Cannon Beach." (<http://ci.cannon-beach.or.us/docs/News/CannonBeach2006.pdf>) (Jul. 15, 2012).
- Dolan, J. D. (1989). "The dynamic response of timber shear walls." Ph.D. thesis, Dept. of Civil Engineering, Univ. of British Columbia, Vancouver, BC, Canada.
- Ellingwood, B. R. (2001). "Earthquake risk assessment of building structures." *Reliab. Eng. Syst. Saf.*, 74(3), 251–262.
- Ellingwood, B. R., Rosowsky, D. V., Li, Y., and Kim, J. H. (2004). "Fragility assessment of light-frame wood construction subjected to wind and earthquake hazards." *J. Struct. Eng.*, 130(12), 1921–1930.
- FEMA. (2008). "Guidelines for design of structures for vertical evacuation from tsunamis." *FEMA P646*, Washington, DC.

- FEMA. (2009). "Quantification of building seismic performance factors." *FEMA P695*, Washington, DC.
- Folz, B., and Filiatrault, A. (2001). "Cyclic analysis of wood shear walls." *J. Struct. Eng.*, 127(4), 433–441.
- Goda, Y. (2010). *Random seas and design of maritime structures*, 3rd Ed., World Scientific, Singapore.
- Kirby, J. T. (2009). "FUNWAVE homepage." (<http://chinacat.coastal.udel.edu/programs/funwave/funwave.html>) (Jan. 14, 2010).
- Koshimura, S., Namegaya, Y., and Yanagisawa, H. (2009a). "Tsunami fragility - A new measure to identify tsunami damage." *J. Disaster Res.*, 4(6), 479–488.
- Koshimura, S., Oie, T., Yanagisawa, H., and Imamura, F. (2009b). "Developing fragility functions for tsunami damage estimation using numerical model and post-tsunami data from Banda Aceh, Indonesia." *Coastal Eng. J.*, 51(3), 243–273.
- Linton, D., Gupta, R., Cox, D., van de Lindt, J. W., Oshnack, M. E., and Clauson, M. (2011). "Evaluation of tsunami loads on wood frame walls at full scale." *J. Struct. Eng.*, 139(8), 1318–1325.
- Liu, P. L.-F. (2009). "COBRAS (Cornell breaking waves and structure)." (<http://ceeserver.cce.cornell.edu/cobras/default.htm>) (Jan. 14, 2010).
- Neelamani, S., Schuttrumpf, H., Muttray, M., and Oumeraci, H. (1999). "Prediction of wave pressures on smooth impermeable seawalls." *Ocean Eng.*, 26(8), 739–765.
- Park, S. (2011). "Understanding and mitigating tsunami risk for coastal structures and communities." Ph.D. thesis, Dept. of Civil and Environmental Engineering, Colorado State Univ., Fort Collins, CO.
- Park, S., and van de Lindt, J. W. (2009). "Formulation of seismic fragilities for a wood-frame building based on visually determined damage indexes." *J. Perform. Constr. Facil.*, 23(5), 346–352.
- Park, S., van de Lindt, J. W., Cox, D., Gupta, R., and Aguiniga, F. (2012). "Successive earthquake-tsunami analysis to develop collapse fragilities." *J. Earthquake Eng.*, 16(6), 851–863.
- Ramsden, J. D. (1996). "Forces on a vertical wall due to long waves, bores, and dry-bed surges." *J. Waterway, Port, Coastal, Ocean Eng.*, 122(3), 134–141.
- Rosowsky, D. V., and Ellingwood, B. R. (2002). "Performance-based engineering of wood frame housing: Fragility analysis methodology." *J. Struct. Eng.*, 128(1), 32–38.
- Shinozuka, M., Feng, M. Q., Lee, J., and Naganuma, T. (2000). "Statistical analysis of fragility curves." *J. Eng. Mech.*, 126(12), 1224–1231.
- Stewart, W. G. (1987). "The seismic design of plywood sheathed shearwalls." Ph.D. thesis, Dept. of Civil Engineering, Univ. of Canterbury, Christchurch, New Zealand.
- USGS. (2011). "U.S. seismic design map." (<https://geohazards.usgs.gov/secure/designmaps/us/>) (Mar. 18, 2011).
- van de Lindt, J. W., and Dao, T. N. (2009). "Performance-based wind engineering for woodframe buildings." *J. Struct. Eng.*, 135(2), 169–177.
- Wilson, J. S., Gupta, R., van de Lindt, J. W., Clauson, M., and Garcia, R. (2009). "Behavior of a one-sixth scale wood-framed residential structure under wave loading." *J. Perform. Constr. Facil.*, 23(5), 336–345.